PLOS ONE

RESEARCH ARTICLE

17-Oxime ethers of oxidized ecdysteroid derivatives modulate oxidative stress in human brain endothelial cells and dose-dependently might protect or damage the blood-brain barrier

Máté Vágvölgyi[1☯], Dávid Laczkó[1☯], Ana Raquel Santa-Maria[2,3], Judit P. Vigh[2,4], Fruzsina R. Walter[2], Róbert Berkecz[5], Mária A. Deli[2], Gábor Tóth[6], Attila Hunyadi[1,7,8]*

1 Institute of Pharmacognosy, University of Szeged, Szeged, Hungary, **2** Institute of Biophysics, HUN-REN Biological Research Centre, Szeged, Hungary, **3** Wyss Institute for Biologically Inspired Engineering at Harvard University, Boston, MA, United States of America, **4** Doctoral School of Biology, University of Szeged, Szeged, Hungary, **5** Institute of Pharmaceutical Analysis, University of Szeged, Szeged, Hungary, **6** NMR Group, Department of Inorganic and Analytical Chemistry, Budapest University of Technology and Economics, Budapest, Hungary, **7** Interdisciplinary Centre of Natural Products, University of Szeged, Szeged, Hungary, **8** HUN-REN-SZTE Biologically Active Natural Products Research Group, Szeged, Hungary

☯ These authors contributed equally to this work.
* hunyadi.attila@szte.hu

Citation: Vágvölgyi M, Laczkó D, Santa-Maria AR, Vigh JP, Walter FR, Berkecz R, et al. (2024) 17-Oxime ethers of oxidized ecdysteroid derivatives modulate oxidative stress in human brain endothelial cells and dose-dependently might protect or damage the blood-brain barrier. PLoS ONE 19(2): e0290526. https://doi.org/10.1371/journal.pone.0290526

Editor: Ahmed E. Abdel Moneim, Helwan University, EGYPT

Received: August 9, 2023

Accepted: January 7, 2024

Published: February 22, 2024

Data Availability Statement: All relevant data are within the manuscript and its Supporting Information files.

Funding: This study was funded by National Research, Development and Innovation Office, Hungary (NKFIH; K134704) and NKFIH and the Ministry of Innovation and Technology, Hungary (TKP2021-EGA-32) awarded to AH; by the Gedeon Richter Plc. Centenarial Foundation Research Grant

Abstract

20-Hydroxyecdysone and several of its oxidized derivatives exert cytoprotective effect in mammals including humans. Inspired by this bioactivity of ecdysteroids, in the current study it was our aim to prepare a set of sidechain-modified derivatives and to evaluate their potential to protect the blood-brain barrier (BBB) from oxidative stress. Six novel ecdysteroids, including an oxime and five oxime ethers, were obtained through regioselective synthesis from a sidechain-cleaved calonysterone derivative **2** and fully characterized by comprehensive NMR techniques revealing their complete ^{1}H and ^{13}C signal assignments. Surprisingly, several compounds sensitized hCMEC/D3 brain microvascular endothelial cells to *tert*-butyl hydroperoxide (tBHP)-induced oxidative damage as recorded by impedance measurements. Compound **8**, containing a benzyloxime ether moiety in its sidechain, was the only one that exerted a protective effect at a higher, 10 μM concentration, while at lower (10 nM–1 μM) concentrations it promoted tBHP-induced cellular damage. Brain endothelial cells were protected from tBHP-induced barrier integrity decrease by treatment with 10 μM of compound **8**, which also mitigated the intracellular reactive oxygen species production elevated by tBHP. Based on our results, 17-oxime ethers of oxidized ecdysteroids modulate oxidative stress of the BBB in a way that may point towards unexpected toxicity. Further studies are needed to evaluate any possible risk connected to dietary ecdysteroid consumption and CNS pathologies in which BBB damage plays an important role.

awarded to FRW; by the European Training Network H2020-MSCA-ITN-2015 (Grant no. 675619) awarded to MD and financing ARSM; by the New National Excellence Program of the Ministry for Culture and Innovation (ÚNKP-22-4-SZTE-169) awarded to MV; by NKFIH, 2022-1.2.6-TÉT-IPARI-TR-2022-00024 awarded to MD and AH; and by NKFIH, cooperative doctoral program (KDP2020-1005968) awarded to AH and DL.

Competing interests: The authors have declared that no competing interests exist.

Introduction

Ecdysteroids are insect molting hormone analogs widespread in the Plant Kingdom, and they have attracted a significant interest due to their non-hormonal anabolic, cytoprotective, and vascular protective activity in mammals. Several recent clinical trials have set their focus on these compounds as potential therapeutic agents in the treatment of sarcopenia (NCT03021798, NCT03452488), or the frequently fatal respiratory deterioration in COVID-19 (NCT04472728).

20-Hydroxyecdysone (20E), the most abundant representative of this compound group, was previously found to exert neuroprotective activity in rodent models of cerebral ischemia/reperfusion [1, 2]. Further, we have recently reported a set of three new, highly oxidized ecdysteroids to protect human brain endothelial cells from oxidative injury [3].

The chemical modification of lipids, proteins, and DNA by reactive oxygen species (ROS) can result in cellular and tissue damage, implicating oxidative stress in the pathogenesis of numerous diseases and injuries affecting almost every organ system. Although oxidative stress and its related disorders are more prevalent in older individuals, environmental factors such as air pollution and UV exposure can expedite the development of these conditions in people of all ages [4]. The impact of oxidative stress on neurodegenerative diseases is of significant interest, as it has been linked to the severity of disease pathology. Biomarkers such as peroxiredoxins and ubiquinone/ubiquinol are found to be elevated in individuals with Alzheimer's disease, Parkinson's disease, and amyotrophic lateral sclerosis, and are associated with cognitive impairment [4–6]. The blood-brain barrier (BBB) plays a crucial role in ROS-mediated injury and neurodegenerative diseases. This barrier is composed of endothelial cells that have a strong and dynamic interaction with the neighbouring cells pericytes and astrocytes. The brain endothelial cells have a unique protection system and it controls the transport of substances in and out of the brain via tight junctions, transport pathways, and efflux proteins [7]. Given that ROS can affect brain endothelial cells and cause BBB disruption, it is crucial to explore whether compounds such as, e.g., ecdysteroids, can provide protection to these cells, promoting BBB protection in the early stages of neurological diseases.

The cytoprotective effect of 20E is at least partly due to its ability to activate protein kinase B (Akt) [8]. In our previous studies on various ecdysteroids as activators of this kinase, we found that calonysterone (**1**), and particularly its side-chain cleaved derivative **2**, are more potent in this regard than 20E in muscle skeletal myotubes [9, 10]. These findings, and the relative ease of performing chemical modifications on the 20-keto group of compound **2** led us to select it as a starting point to create a new cohort of potentially cytoprotective semi-synthetic ecdysteroid derivatives.

Our previous studies on ecdysteroid oximes and oxime ethers revealed that poststerone, the side-chain cleaved derivative of 20E, can be transformed into 20-oximes and oxime ethers in a regioselective manner [11]. This opened way to a synthetic strategy to prepare ecdysteroid derivatives with a modified, nitrogen-containing side-chain.

Inspired by the neuro- and cerebrovascular protective activity of natural ecdysteroids against ROS, in this work it was our aim to prepare a set of sidechain-cleaved and oxime ether-containing sidechain-modified derivatives of calonysterone (**1**), and to evaluate the compounds' bioactivity as potential BBB protecting candidates.

Results and discussion

Chemistry

Oxidative sidechain cleavage. The regioselective oxidative cleavage between the 20,22-diol to eliminate the sterol side chain at the C-17 position of calonysterone **1** was carried

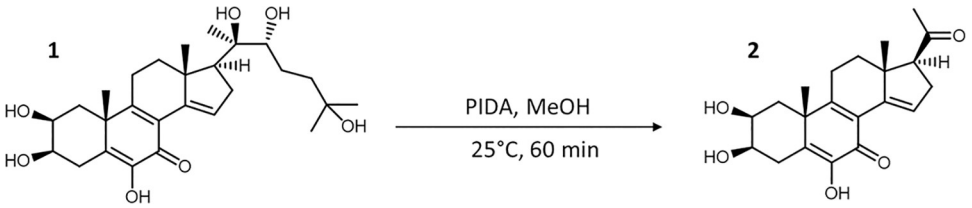

Fig 1. Oxidative cleavage of the sterol sidechain of calonysterone (1).

https://doi.org/10.1371/journal.pone.0290526.g001

out with the hypervalent iodine reagent (diacetoxyiodo)benzene (PIDA), which had been successfully used for the similar purpose in the case of 20-hydroxyecdysone [10]. According to our previous results, using this reagent leads to a significantly better yield than [bis(trifluoroacetoxy)iodo]benzene (PIFA), a more aggressive oxidant [10]. Full conversion was achieved within an hour. After neutralization and evaporation of the solvent, normal-phase chromatography was used for purification; this was a more practical choice than reverse-phase separation due to its higher loading capacity and milder solvent evaporation conditions. Outline of the reaction is shown in (Fig 1).

Regioselective formation of 20-oxime or -oxime ether function. Previously, we reported that the 6-enone function of poststerone is relatively less reactive for oxime formation than its 17-oxo group [12], therefore it was postulated that a similar regioselective oximation should be straightforward also for compound **2**.

At first, we performed small-scale (with approx. 10 mg of substrate) test reactions monitored by TLC in every 10 minutes, and we found that all reactions reached full conversion within 40 minutes. Our experiments included the use of either pyridine or ethanol as solvent, and our experience showed that the reactions proceeded in both solvents with nearly identical results. Therefore, we chose ethanol considering its lower boiling point that makes it easier to evaporate during the work-up. After the transformations, the solvent was evaporated on a rotary vacuum evaporator and liquid-liquid extraction was performed with water and ethyl acetate. Outline of the synthesis and structure of the products is shown in (Fig 2).

Following this strategy, a total of six new ecdysteroid C-20 oxime and oxime ether derivatives were synthesized from larger-scale aliquots of compound **2**. After pre-purification of the synthesized materials, their HPLC chromatograms were recorded, which was accompanied by the mapping of the eluent systems for their preparative RP-HPLC purification. To improve sample solubility for preparative RP-HPLC, a 3:7 (v/v) ratio solvent mixture of dimethyl sulfoxide (DMSO) and acetonitrile was used.

Structure elucidation. We have recently reported the structure elucidation and complete ^{1}H and ^{13}C signal assignment of compound **1** [9] and the sidechain-cleaved calonysterone derivative **2** [10]. Structure elucidation of the new compounds **3–8** (Fig 2) was performed based on the molecular formulas obtained by HRMS and on detailed NMR studies. The

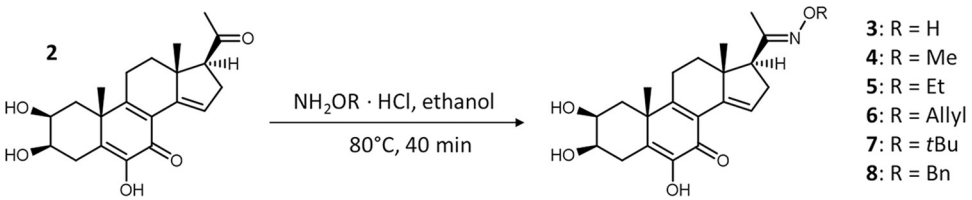

Fig 2. Synthesis of oxime (3) and oxime ether (4–8) derivatives of compound 2.

https://doi.org/10.1371/journal.pone.0290526.g002

obtained HRMS data verified that our synthetic oximation procedure was regioselective in each case, and the reaction took place at either the 6- or 20-carbonyl groups of the substrate. The location and identity of the newly formed functions was determined by means of comprehensive one- and two-dimensional NMR methods using widely accepted strategies [13, 14].

^{1}H NMR, ^{13}C DeptQ, edHSQC, HMBC, one-dimensional selective ROESY (Rotating frame Overhauser Enchancement Spectroscopy) spectra (τ_{mix}: 300ms) were utilized to achieve complete ^{1}H and ^{13}C signal assignment. It is worth mentioning that due to the molecular mass of compounds **3–8** (374–464 Da) the signal/noise value of the selective ROE experiments strongly exceeds that of the selective NOEs. ^{1}H assignments were accomplished using general knowledge of chemical shift dispersion with the aid of the ^{1}H-^{1}H coupling pattern. ^{1}H and ^{13}C chemical shifts (600 and 150 MHz, respectively), multiplicities and coupling constants of compounds **3–8** are compiled in (Table 1). Since the stereostructure of the steroid frame is identical within these compounds, we described the multiplicity and *J* coupling constants only for 3. The characteristic NMR (S1–S20 Figs in S1 File) and HRMS (S21–S26 Figs in S1 File) spectra of compounds **3–8** are presented as Supporting Information. To facilitate the understanding of the ^{1}H and ^{13}C signal assignments, the compounds' structures are also depicted on the spectra.

Only one set of signals appeared in the ^{1}H and ^{13}C NMR spectra of each compound, indicating that the regioselective oximation led to the isolation of one stereoisomer for each. The measured Δδ 55 ppm diamagnetic change of δC-20 (211 → 156 ppm) supported the C=O → C=NOR conversion [11]. During the NMR study of isomeric Z/E 6-oxime derivatives of 20-hydroxyecdysone 2,3;20,22-diacetonide the chemical shift of α carbon atoms (δC-5 and δC-7) in the syn position with respect to the oxime hydroxyl group exhibits a significant (Δδ syn-anti ~ 5 ppm) diamagnetic shift, which was successfully utilized for differentiation of (Z/E) isomers [12]. In the present case for compounds **3–8**, due to the absence of exact data of Δδ syn-anti parameters for the C-21 and C-17 signals, the unambiguous identification of the E/Z isomerism in this way was not possible. To overcome this problem, we utilized a series of selective ROESY experiments on the CH_3-21 signals (S1, S8 and S13 Figs in S1 File), and the detected steric responses unequivocally proved the *E* configuration of the oxime moiety. By introducing the 1D selROE spectrum on H_3-21 into the edited HSQC experiment (S3, S8 and S13 Figs in S1 File), the ROE signals allowed identifying the corresponding C–H cross-peaks. The quaternary carbon signals were identified from the HMBC spectra, for which the HMBC responses over two and three bonds of H_3-19, H_3-18, and H_3-21 were very effective (S4, S9 and S14 Figs in S1 File).

Biology

Impedance measurements. As a simplified model of the BBB the hCMEC/D3 human brain endothelial cell line was used. This widely employed and well characterized model [15, 16] expresses many important BBB characteristics including junctional proteins, metabolic enzymes, efflux and influx transporters [17]. We evaluated the effect of the compounds on the viability of hCMEC/D3 cells using impedance measurements. Initially, we tested concentration ranges of 0.01–10 μM for all compounds, and no notable changes in cell viability were observed, except for compounds **3**, **4** and **8** (Supporting Information, S27 Fig in S1 File). Although we monitored all concentrations for 24 hours, we observed that the onset of the effects for all compounds was at the 4-hour time point. Therefore, we have focused our results on the 4h time point. For compound **3** we could observe a significant cell index decrease for 10 μM concentration, however, for compound **4** a significant increase for 1 μM concentration was observed (Supporting Information, S27 Fig in S1 File). Notably, compound **8** exhibited

Table 1. ^{1}H and ^{13}C chemical shifts, multiplicities and coupling constants of compounds 3–8 in dmso-d_6.

	3			4		5		6		7		8	
no.	^{1}H	*J* (Hz)	^{13}C	^{1}H	^{13}C	^{1}H	^{13}C	^{1}H	^{13}C	^{1}H	^{13}C	^{1}H	^{13}C
1β	2.29	dd; 14.0;2.9	41.7	2.28	41.7	2.28	41.7	2.28	41.7	2.29	41.7	2.28	41.7
α	1.27	dd; 14.0;3.3		1.25		1.26		1.28		1.26		1.25	
2	3.84		68.3	3.84	68.4	3.83	68.3	3.83	68.3	3.83	68.3	3.83	68.3
3	3.33		72.2	3.33	72.3	3.33	72.2	3.35	72.2	3.33	72.2	3.35	72.2
4β	2.37	t; 12.1	27.0	2.37	27.1	2.37	27.0	2.37	27.0	2.37	27.0	2.37	27.0
α	2.92	ddd; 12.1;4.8;1.2		2.92		2.92		2.92		2.92		2.92	
5			133.1		133.2		133.1		133.1		133.1		133.2
6			142.8		142.9		142.8		142.8		142.8		142.8
7			179.6		179.6		179.5		179.5		179.5		179.5
8			123.1		123.2		123.1		123.1		123.1		123.1
9			164.3		164.4		164.3		164.3		164.2		164.3
10			41.1		41.2		41.1		41.1		41.1		41.1
11β	2.52		24.0	2.52	24.1	2.53	24.0	2.52	24.0	2.54	24.0	2.50	24.0
α	2.63	ddd; 19.0;5.0;~1		2.63		2.63		2.63		2.63		2.61	
12β	2.08		34.9	2.06	34.9	2.06	34.8	2.06	34.8	2.07	34.9	2.03	34.8
α	1.53	td; 12.5;5.0		1.51		1.52		1.52		1.53		1.51	
13			46.5		46.7		46.6		46.7		46.6		46.7
14			140.2		140.2		141.0		140.1		140.1		140.1
15	6.79	t; 2.7	126.3	6.78	126.2	6.78	126.2	6.78	126.1	6.78	126.2	6.77	126.1
16β	2.93		32.7	2.90	32.6	2.91	32.6	2.90	32.5	2.96	32.7	2.90	32.5
α	2.26	ddd; 16.9;7.5;~3		2.26		2.26		2.26		2.29		2.29	
17	2.57	dd; 10.6;7.5	55.9	2.57	55.5	2.57	55.5	2.58	55.5	2.58	55.9	2.58	55.5
18	0.68		18.3	0.68	17.3	0.69	17.3	0.63	17.3	0.68	17.3	0.63	17.3
19	1.40		27.3	1.38	27.3	1.40	27.2	1.39	27.2	1.40	27.2	1.39	27.2
20			154.8		156.6		156.1		156.7		154.2		157.1
21	1.81		15.1	1.82	15.7	1.83	15.7	1.88	15.7	1.81	15.7	1.88	15.9
22				3.76	61.1	4.01	68.27	4.51	73.7		77.2	5.05	74.8
23						1.17	14.9	5.95	135.2	1.23	27.7		138.6
24								5.24 5.16	116.9	1.23	27.7	7.34	128.0
25										1.23	27.7	7.34	128.4
26												7.27	127.7
27												7.34	128.4
28												7.34	128.0
HO-2		d; 2.9		3.84									
HO-3		d; 5.6		4.95									

https://doi.org/10.1371/journal.pone.0290526.t001

the highest and most significant activity. At concentrations of 0.01, 0.1, 1, and 10 μM, it demonstrated a positive effect on barrier integrity. As compound **8** demonstrated the highest activity, we decided to investigate whether it also promotes a protective effect against oxidative stress. Excessive ROS resulting from oxidative stress can cause disruption of the BBB by compromising the antioxidant defense system. The damaging effects of ROS on cellular components such as proteins, lipids, and DNA can lead to the modulation of tight junctions, activation of matrix metalloproteinases, and upregulation of inflammatory molecules, all of which can contribute to BBB damage [18]. Tert-butyl hydroperoxide (tBHP) is known to induce cellular damage by generating high levels of ROS [19]. Therefore, to assess the protective effects

of the compound against ROS-induced damage, we treated cells with tBHP (350 μM) alone or in combination with 0.01, 0.1, 1 and 10 μM of compound **8**. We identified the optimal concentration of tBHP by testing different concentrations and selected 350 μM, which did not decrease the cell index below ~50% in our previous work. This concentration was then used for the cell viability assay.

We can observe a significant decrease in cell viability by a total of ca. 60% in the presence of tBHP compared to the control group (Fig 3B and 3C), indicating tBHP-induced oxidative damage on the cells. Treatment of 10 μM of compound **8** resulted in a significant and steady increase of cell impedance, i.e., it was able to protect the cells efficiently from the harmful effects of tBHP. These findings suggest that the compound might have a protective effect against cellular damage induced by ROS (Fig 3B and 3C). However, at smaller, 10 nM, 100 nM, and 1 μM concentrations a surprising opposite effect was observed. At lower concentrations for 6h or longer incubation, compound **8** increased tBHP-induced toxicity, leading to a disruption of the cellular layer (Fig 3C). We also tested compounds **4** and **6** (3 and 10 μM) in combination with 350 μM of tBHP, and both significantly increased oxidative damage at these concentrations (Supporting Information, S28 Fig in S1 File).

The use of impedance-based monitoring to assess brain endothelial cell function is crucial as it not only measures the number of viable cells but also provides valuable information on the integrity of the cell layer and the extent of barrier damage. This method has been shown to be relevant to evaluate barrier integrity and the overall health of brain endothelial cells [3, 20, 21]. There is evidence indicating that oxidative stress plays a crucial role in the induction of BBB damage [7]. The present study provided evidence that treatment with tBHP resulted in brain endothelial damage, which was manifested by a decrease in cell and barrier integrity in certain concentrations of the compounds tested. However, co-treatment with compound **8** significantly altered this effect, leading to the prevention or promotion of oxidative barrier damage. During the 24h-long monitoring of the cell index, a clear concentration-dependent distinction could be made between the protective or damaging effect. Since no data are available on the pharmacokinetics of compound **8**, it is not possible to evaluate if a 10 μM plasma level is a realistic concentration in vivo or not. On the other hand, the low-concentration effect of compound **8** to sensitize the BBB to oxidative stress clearly raises a warning concerning its value as a lead compound.

In the broader context, it may be worth stressing that the herein reported compounds are semi-synthetic ecdysteroids that contain oxime ether moieties in their sidechain. This functional group is not expectable to occur in natural ecdysteroids or their metabolites, therefore our results do not directly imply any risk connected to phytoecdysteroid consumption. In our previous study on minor phytoecdysteroids [3], only protective effects were observed. Nevertheless, considering that hardly anything is known about ecdysteroids' bioactivity in relation with the BBB, further studies are needed to evaluate related drug discovery potential and/or risks of this compound family.

Reactive oxygen species measurement. To complete the data, ROS production was also measured in human brain endothelial cells after 0.01–10 μM compound **8** treatment alone or in combination with tBHP for 4 hours. It was confirmed that 350 μM tBHP significantly increased the ROS production, four times to the level of the control group (Fig 4). Addition of 10 μM of compound **8** significantly decreased the tBHP-induced ROS production compared to tBHP treatment alone, although it was still 3 times higher than the control. Treatment with compound **8** alone did not affect ROS production. Compound **8** at lower concentrations (0.01–1 μM) did not decrease ROS production except for 0.1 μM treatment which had a small but significant protective effect against the tBHP induced stress.

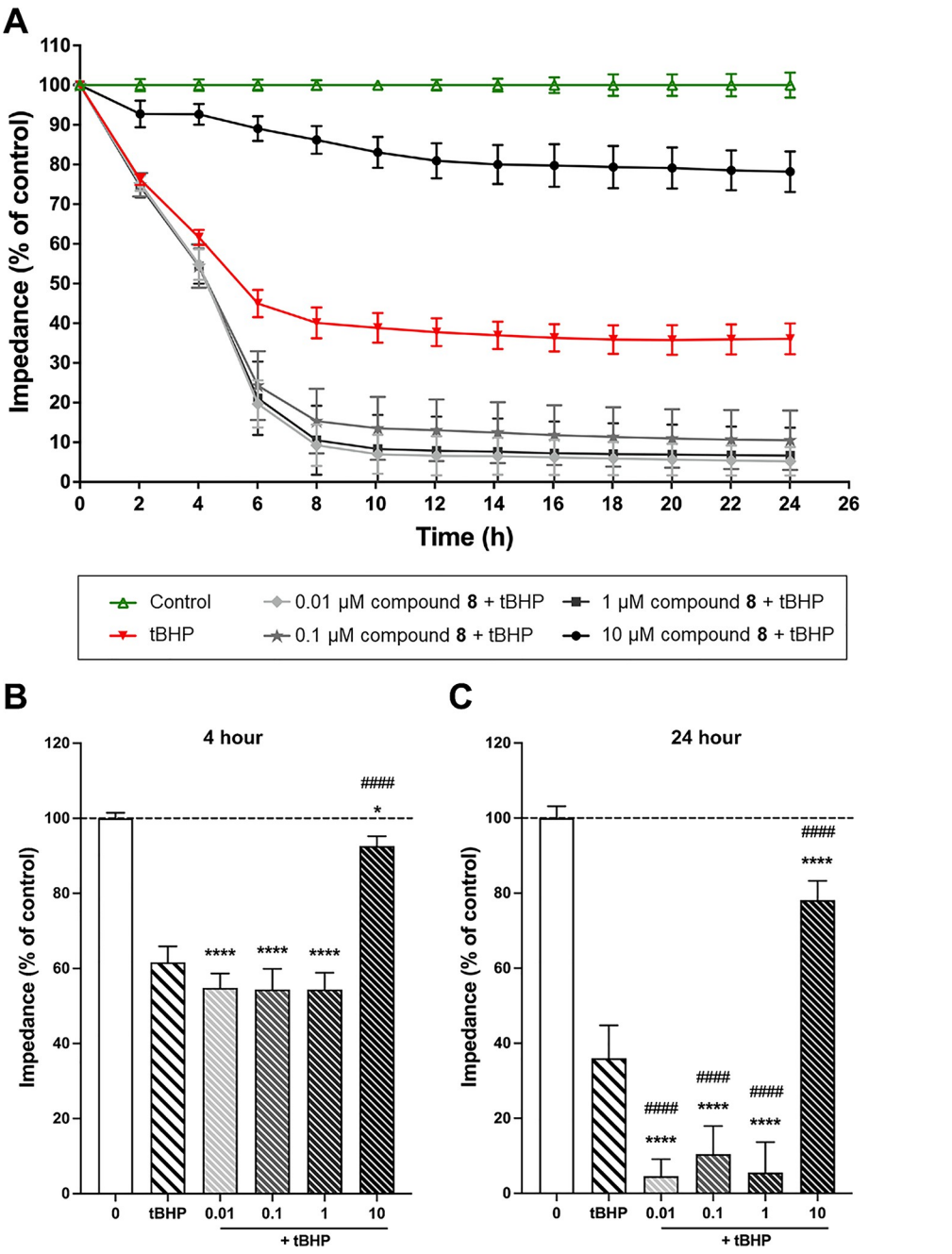

Fig 3. The effects of compound 8 at concentrations of 0.01, 0.1, 1, and 10 μM treatment on human brain microvascular endothelial cells (hCMEC/D3) were evaluated using impedance-based assays to assess cell viability and barrier integrity in the absence and presence of oxidative stress promoted by tert-butyl hydroperoxide (tBHP). **A**: Time-dependent impact of **8** on cell viability following co-treatment with tBHP (350 μM). **B**: Impact of **8** on cell viability at 4 hours co-treatment with tBHP (350 μM). **C**: Impact of **8** on cell viability at 24 hours co-treatment with tBHP (350 μM). The data are presented as the mean ± standard deviation (SD) and were obtained from a minimum of two independent experiments (n = 2–3) with 3–9 technical replicates. Data analysis was performed using one-way analysis of variance (ANOVA) followed by Dunnett's multiple comparisons test. The results were statistically significant with $^{*}p < 0.05$, $^{****}p < 0.0001$, compared to the control group, and $^{\#\#\#\#}p < 0.0001$, compared to the tBHP group.

https://doi.org/10.1371/journal.pone.0290526.g003

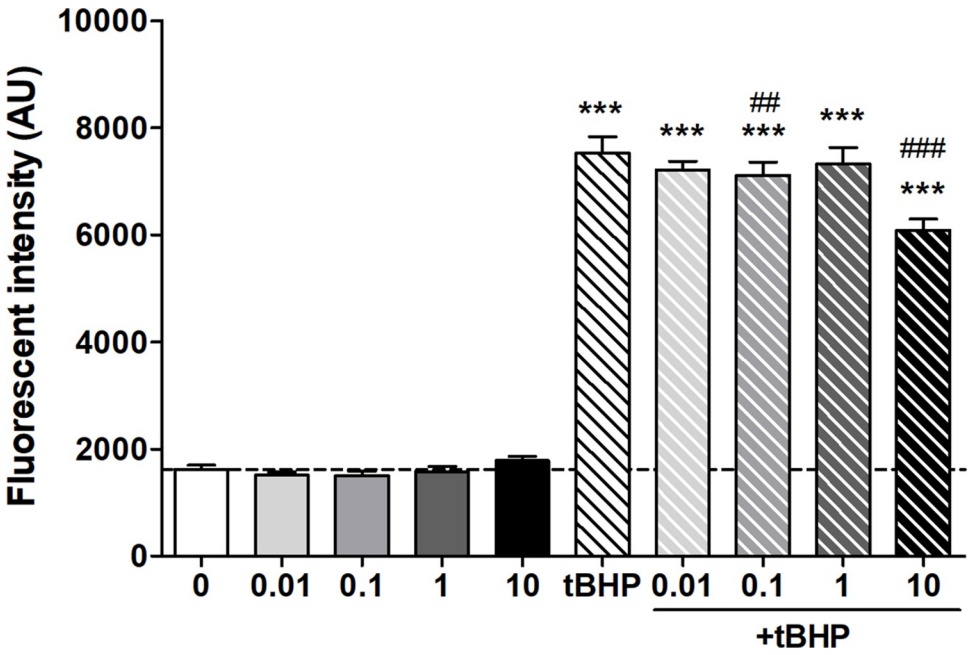

Fig 4. Reactive oxygen species (ROS) measurement in human brain microvascular endothelial cells (hCMEC/D3) after 4-hour treatment with 0.01–10 μM compound 8 in the absence and presence of oxidative stress promoted by tert-butyl hydroperoxide (tBHP, 350 μM). Data is given in fluorescent intensity corresponding to ROS amount produced intracellularly measured by DCFDA assay. Data are presented as mean ± standard deviation (SD; n = 7–8). Data analysis was performed using one-way analysis of variance (ANOVA) followed by Bonferroni's multiple comparisons test. Statistical significance: $^{***}p < 0.001$, compared to the control group, $^{\#\#}p < 0.01$; $^{\#\#\#}p < 0.001$, compared to the tBHP group.

https://doi.org/10.1371/journal.pone.0290526.g004

Barrier integrity tests. To confirm the protective effect of compound **8** at 10 μM concentration against tBHP-induced ROS damage transendothelial electrical resistance (TEER) and permeability measurements for fluorescent marker molecules were performed. For the permeability assay paracellular permeability marker 4 kDa FITC-dextran (FD4) and Evans blue-labeled albumin (EBA, 67 kDa), a marker of adsorption-mediated transcytosis, were used. Changes in intercellular connections were visualized by immunocytochemistry for cell junction associated molecules zonula occludens-1 (ZO-1) and β-catenin (Fig 5). All experiments were performed at the 4-hour treatment endpoint. We found that tBHP decreased the TEER and increased the FD4 permeability of the brain endothelial cell monolayer. This barrier integrity decreasing effect was rescued by the co-incubation with 10 μM compound **8**. Treatment with tBHP alone or in combination with compound **8** had no significant effect on the EBA permeability. Compound **8** alone decreased the permeability of the BBB model both for FD4 and EBA compared to the control indicating a barrier tightening effect. These data corroborate the impedance measurements performed with compound **8** alone (S27 Fig in S1 File). After the barrier integrity measurements cells were fixed and stained for junctional proteins. Staining for ZO-1 and β-catenin in the control group showed elongated cell shape and a confluent cell layer typical for hCMEC/D3 cultures. The morphology of brain endothelial cells treated with compound **8** was similar to the control. The barrier integrity decreasing effect of tBHP was also visible on the cellular morphology: irregular cell borders and discontinuity in the staining could be observed. Co-treatment with compound **8** resulted in the recovery of the brain endothelial cell morphology (Fig 5).

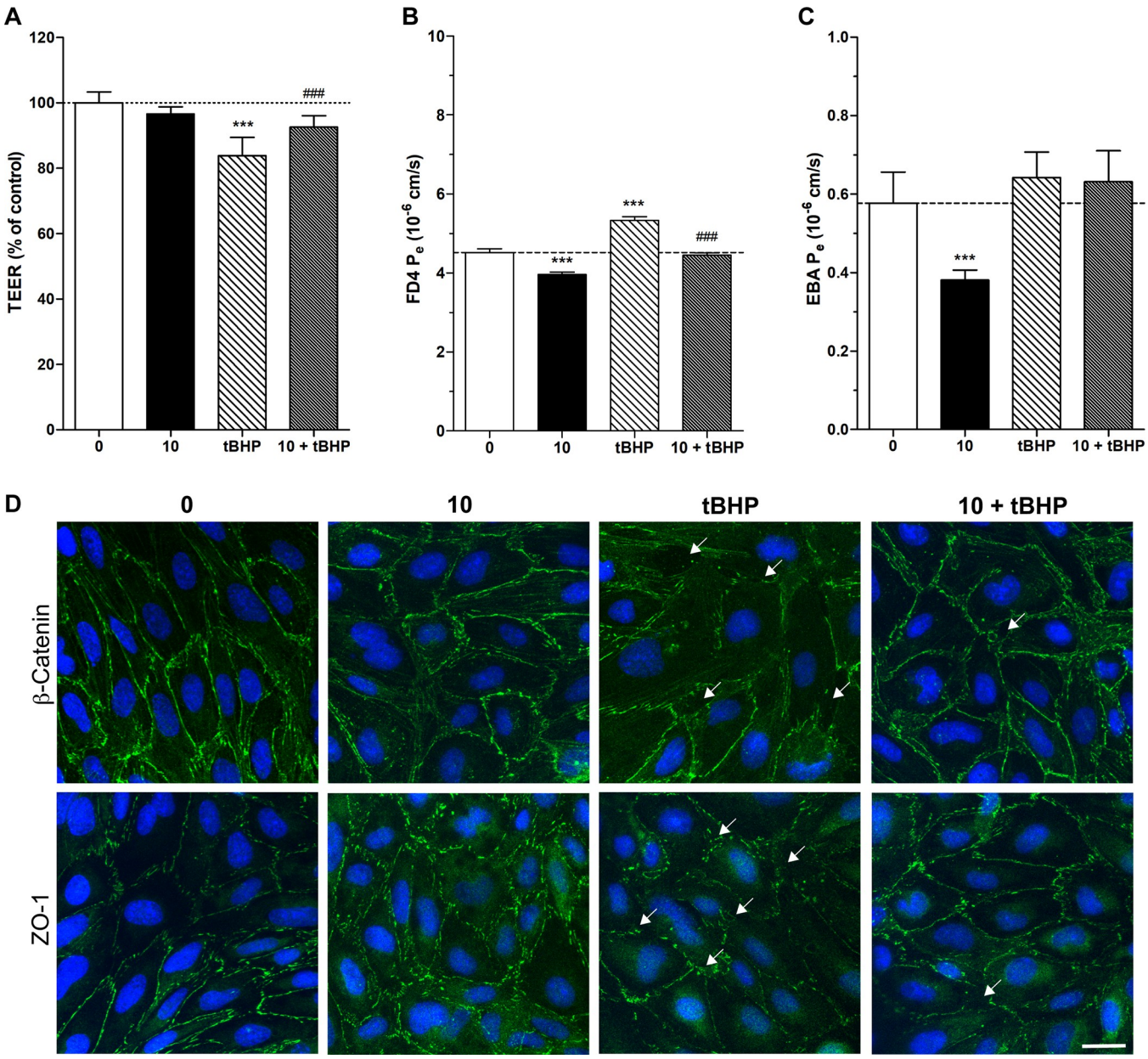

Fig 5. Effects of compound 8 (10 μM) on the barrier integrity of human brain microvascular endothelial cells (hCMEC/D3) in the absence and presence of oxidative stress promoted by tert-butyl hydroperoxide (tBHP, 350 μM). All treatments were performed for 4 hours. **A**: Transendothelial electrical resistance (TEER) measurement. **B**: Permeability measurement for the paracellular marker molecule FITC-dextran 4 kDa (FD4). **C**: Permeability measurement for the transcellular marker molecule Evans blue labeled-albumin (EBA, 67 kDa). Data are presented as mean ± standard deviation (SD; n = 4). Data analysis was performed using one-way analysis of variance (ANOVA) followed by Bonferroni's multiple comparisons test. Statistical significance: $^{***}p < 0.001$, compared to the control group, and $^{###}p < 0.001$, compared to the tBHP group. **D:** Immunocytochemistry for β-catenin and zonula occludens-1 (ZO-1) junctional associated molecules. Green: junctional staining. Blue: cell nuclei. Bar: 20 μm.

https://doi.org/10.1371/journal.pone.0290526.g005

Experimental

Materials and methods

Chemistry. All solvents and reagents were purchased from Sigma-Aldrich (Merck KGaA, Darmstadt, Germany) and were used without any further purification. The progress of the

reactions was monitored by thin layer chromatography (TLC) on Kieselgel 60F254 silica plates purchased from Merck (Merck KGaA, Darmstadt, Germany). The examination of the plates was carried out under UV illumination at 254 and 366 nm.

The purification of calonysterone was performed by centrifugal partition chromatography on a 250 ml Armen Spot instrument (Gilson Inc., Middleton, WI, USA). The flash chromatographic purification of compound **2** was carried out on a Combiflash Rf+ instrument (Teledyne ISCO, Lincoln, NE, USA) equipped with diode array and evaporative light scattering detection (DAD-ELSD), and commercially available prefilled RediSep columns (Teledyne ISCO, Lincoln, NE, USA) were utilized. For the analysis of the compounds, we used a dual-pump Jasco HPLC instrument (Jasco International Co. Ltd., Hachioji, Tokyo, Japan) equipped with an "MD-2010 Plus" PDA detector. The analytical-scale separations were performed on a Phenomenex Kinetex Biphenyl 100A 5μ 250x4.6 mm (Torrence, CA, USA) HPLC column. The separation of compound 4–8 was performed on an Armen "Spot Prep II" preparative chromatographic apparatus (Gilson Inc., Middleton, WI, USA) equipped with a dual-wavelength UV detector and four individual solvent pumps. The RP-HPLC purification of the ecdysteroid products was carried out with adequately chosen isocratic eluent mixtures of acetonitrile and water.

Isolation of calonysterone (1). A commercially available extract prepared from *Cyanotis arachnoidea* roots was purchased from Xi'an Olin Biological Technology Co., Ltd. (Xi'an, China) [22], and subjected to a chromatographic purification to obtain the starting material calonysterone (**1**) as published before [23]. Briefly, 5.46 kg of extract was percolated with 15.5 L of methanol, and after evaporation of the solvent, the dry residue (700 g) was subjected to further separation by a multi-step chromatographic fractionation through silica gel. The final purification of **1** was carried out using centrifugal partition chromatography in ascending mode with a biphasic solvent system of *n*-hexane–ethyl acetate–methanol–water (1:5:1:5, v/v/v/v) [23].

Preparation of compound 2 via the oxidative side-chain cleavage of calonysterone (1). An aliquot of 2 g of calonysterone (**1**) was dissolved in 500 ml of methanol. One equivalent (1.34 g) of PIDA was added, and the reaction mixture was stirred for 60 minutes at room temperature. The solution was then neutralized with 10% aq. $NaHCO_3$, and the solvent was evaporated under reduced pressure on a rotary evaporator. Subsequently, the residue was re-dissolved in acetone and adsorbed on 10 g of silica gel for dry loading. The product was purified by flash chromatography on a 24 g silica column (flow rate 35 ml/min, run time: 60 min) with a gradient of dichloromethane (A) and methanol (B), from 0% to 15% of solvent B in A. The separation afforded compound **2** in a yield of 45.5%.

General procedure for the synthesis of sidechain cleaved calonysterone 20-oxime and oxime ether derivatives 3–8. A 120 mg aliquot of compound **2** (0,34 mmol) was dissolved in ethanol (20 ml) and depending on the functional group to be coupled, 120 mg of hydroxylamine hydrochloride (compound **3**) or alkoxyamine hydrochloride (compounds **4**–**8**) was added to the solution under stirring. After 40 minutes of stirring at 80˚C the solution was evaporated to dryness under reduced pressure. After water addition to the dry residue (100 ml), the aqueous solution was extracted three times with ethyl acetate (3x100 ml) and the combined organic phase was dried over anhydrous Na_2SO_4. Subsequently, the solution was filtered, and the solvent was evaporated under reduced pressure. The purification of the mixture was implemented by preparative RP-HPLC to afford the corresponding ecdysteroid product.

Procedures for structure elucidation of the obtained products. HR-MS analysis of the compounds was carried out on an Agilent 1100 LC-MS instrument (Agilent Technologies, Santa Clara, CA, USA) coupled with Thermo Q-Exactive Plus orbitrap spectrometer (Thermo Fisher Scientific, Waltham, MA, USA) used in positive ionization mode. Regarding the samples, 100 μg/ml solutions were prepared with acetonitrile solvent containing 0.1% formic acid.

^{1}H NMR, ^{13}C DeptQ, edHSQC, HMBC, and one-dimensional selective ROESY spectra (τ_{mix}: 300ms) were recorded at 295 K on a Bruker Avance III HD 600 (Billerica, MA, USA; 600 and 150 MHz for ^{1}H and ^{13}C NMR spectra, respectively) spectrometer equipped with a Prodigy cryo-probehead. The pulse programs were taken from the Bruker software library (TopSpin 3.5). ^{1}H assignments were accomplished using general knowledge of chemical shift dispersion with the aid of the ^{1}H-^{1}H coupling pattern (^{1}H NMR spectra). DMSO-d_6 were used as the solvent and tetramethylsilane (TMS) as the internal standard and amounts of approximately 1–5 mg of compound was dissolved in 0.1 ml of solvent and transferred to 2.5 mm Bruker MATCH NMR sample tube (Bruker). Chemical shifts (δ) and coupling constants (*J*) are given in ppm and in Hz, respectively. To facilitate the understanding of the ^{1}H and ^{13}C signal assignments, the structures are also depicted on the spectra (Supporting Information, S1–S20 Figs in S1 File).

Compound 3: off-white, solid; isolated yield: 49.4 mg (39.5%); RP-HPLC purity: 98.1%; for ^{1}H and ^{13}C NMR data, see Table 1 and S1–S4 Figs in S1 File; HR-MS: $C_{21}H_{27}NO_5$, $[M+H]^+$ Calcd.: 374.19730, found: 374.19696 (S21 Fig in S1 File).

Compound 4: off-white, solid; isolated yield: 33.1 mg (25.5%); RP-HPLC purity: 99.1%; for ^{1}H and ^{13}C NMR data, see Table 1 and S5–S9 Figs in S1 File; HR-MS: $C_{22}H_{29}NO_5$, $[M+H]^+$ Calcd.: 388.21185, found: 388.21208 (S22 Fig in S1 File).

Compound 5: off-white, solid; isolated yield: 50.6 mg (37.7%); RP-HPLC purity: 98.0%; for ^{1}H and ^{13}C NMR data, see Table 1, and S10–S14 Figs in S1 File; HR-MS: $C_{23}H_{31}NO_5$, $[M+H]^+$ Calcd.: 402.22750, found: 402.22795 (S23 Fig in S1 File).

Compound 6: off-white, solid; isolated yield: 52.1 mg (37.7%); RP-HPLC purity: 98.9%; for ^{1}H and ^{13}C NMR data, see Table 1, and S15, S16 Figs in S1 File; HR-MS: $C_{24}H_{31}NO_5$, [M+H] + Calcd.: 414.22750, found: 414.22808 (S24 Fig in S1 File).

Compound 7: off-white, solid; isolated yield: 27.8 mg (19.4%); RP-HPLC purity: 97.4%; for ^{1}H and ^{13}C NMR data, see Table 1, and S17, S18 Figs in S1 File; HR-MS: $C_{25}H_{35}NO_5$, $[M+H]^+$ Calcd.: 430.25880, found: 430.25890 (S25 Fig in S1 File).

Compound 8: off-white, solid; isolated yield: 54.9 mg (35.3%); RP-HPLC purity: 97.1%; for ^{1}H and ^{13}C NMR data, see Table 1, and S19, S20 Figs in S1 File; HR-MS: $C_{28}H_{33}NO_5$, $[M+H]^+$ Calcd.: 464.24315, found: 464.24351 (S26 Fig in S1 File).

Biology

Human brain microvascular endothelial cell line (hCMEC/D3) as a blood-brain barrier cell culture model. The hCMEC/D3 human brain microvascular endothelial cell line was obtained from Merck Millipore (Germany). To maintain the cells' brain endothelial-like features, we used cells under passage number 35 [16]. Cells were grown in dishes coated with rat tail collagen and maintained in an incubator at 37˚C with 5% CO_2. The basal medium used was MCDB 131 (Pan Biotech, Germany) supplemented with 5% fetal bovine serum, GlutaMAX (100 ×, Life Technologies, USA), lipid supplement (100 ×, Life Technologies, USA), 10 μg/ml ascorbic acid, 550 nM hydrocortisone, 37.5 μg/ml heparin, 1 ng/ml basic fibroblast growth factor (Roche, USA), 5 μg/ml insulin, 5 μg/ml transferrin, 5 ng/ml selenium supplement (100x, PanBiotech), 10 mM HEPES, and gentamycin (50 μg/ml). We changed the medium every two or three days. When the cultures reached almost 90% confluence, we passaged them to rat tail collagen-coated 96-well plates (E-plate, Agilent, USA) for impedance measurement assays, cell culture inserts (0.4 μm pore size, cellQUART, Sabeu, Germany) for barrier integrity assays and 96-well black-wall plates (Corning, USA) for ROS measurement. Before each experiment, the medium was supplemented with 10 mM LiCl for 24 hours to improve BBB properties [17]. For further characterization and gene expression studies please see [15–17, 24].

Impedance measurements for cell viability assays. The impedance of brain endothelial cells was assessed using the real-time cell electronic sensing analysis (RTCA), which has been shown to correlate with cell number, adherence, growth, and viability [25]. The hCMEC/D3 cells were seeded in 96-well E-plates (Agilent, USA) with golden electrodes at the bottom of the plate at a density of 5×10^3 cells per well and incubated in a CO_2 incubator at 37˚C for 5–6 days, until cell growth reaches a plateau phase. The medium was changed every two days. Once the cells reached a stable growth, they were treated with compounds **2**–**8** at concentrations ranging from 0.01 to 10μM, and their impedance was monitored for 24 hours. From the impedance changes we can interpret the effects of the compounds on cell viability, cell adhesion to the plate or the strength of intercellular junctions [26]. Triton X-100 was used to determine 100% toxicity. After 24-hours measurement, we found that the compounds exhibited the highest level of activity after 4-hours of treatment. As a result, we decided to focus our treatments at this time point.

Preparation of stock and working solutions for the cellular assays. The compounds were obtained as dry powder and stored at -20˚C until use. Stock solutions were prepared by diluting the compounds in DMSO to a final concentration of 10 mM and stored at -20˚C. Working solutions were freshly prepared by diluting the stock solutions in cell culture medium to obtain a concentration range of 0.01–10 μM.

Induction of oxidative stress by *tert*-butyl hydroperoxide. The oxidative compound tert-butyl hydroperoxide (tBHP) can cause cell death through apoptosis or necrosis by generating tert-butoxyl radicals via iron-dependent reactions. This results in lipid peroxidation, depletion of intracellular glutathione, and modification of protein thiols, leading to loss of cell viability [19, 27, 28]. To determine a concentration that would result in approximately 50% cell viability loss, various concentrations of tBHP were tested ranging from 1–1000 μM in preliminary experiments [3]. Based on these results, 350 μM tBHP was found to be effective and was used in combination with the selected concentrations of the compounds to test for potential protective effects.

Barrier integrity assays. TEER measurements reflect the permeability of intercellular tight junctions for ions [26]. Resistance was measured using the EVOM (Endothelial Volt-Ohm Meter) instrument combined with chopstick electrodes (World Precision Instruments, USA). TEER was expressed relative to the surface area ($\Omega \times cm^2$). TEER values of cell-free inserts (10.41 ±0.48 $\Omega \times cm^2$, n = 16) were subtracted from the measured data and normalized to the control group. Permeability experiments were performed as described previously [29]. To measure the flux of paracellular permeability the fluorescent marker FD4 was used. Transcellular permeability was estimated by the transfer of EBA dye across endothelial cell layers. hCMEC/D3 cells were passaged onto cellQuart culture inserts and grown for 5 days. Cells were treated for 4 hours then permeability assays were performed [29]. After the assay the fluorescent intensity of the marker molecules in the upper and lower cell culture insert compartments were determined by a microplate reader (Fluostar Optima, BMG Labtech, Germany; emission wavelength: 485 nm, excitation wavelength: 520 nm). Flux across cell-free inserts was also measured. Endothelial permeability coefficient was calculated as described in an earlier publication of the team [30].

ROS measurement. Total ROS generated after the treatments with compound **8** and tBHP alone or in combination was measured by a fluorometric detection probe, chloromethyl-dichloro-dihydro-fluorescein diacetate (DCFDA) assay (Life Technologies, USA) as described earlier [29]. DCFDA diffuses into the cells and becomes deacetylated by intracellular esterases yielding a fluorescent molecule, which can be detected (Fluostar Optima, ex. 485 nm/em. 520 nm). hCMEC/D3 cells were cultured in black-wall 96-well plates (Corning) until confluency and were treated for 4 hours. In the last 1 hour of the treatment DCFDA was added to

the cells and fluorescence was measured in real time. The fluorescent values detected are presented as arbitrary units.

Statistics. The mean ± SD values were used to present the data. The statistical significance between different treatment groups was assessed using one-way ANOVA, followed by Bonferroni's multiple comparison post-tests (GraphPad Prism 9.0; GraphPad Software, USA). At least four parallel samples were used, and changes were considered statistically significant when $p < 0.05$.

Conclusions

In this study, we have prepared a sidechain cleaved, oxidized ecdysteroid and six of its oxime or oxime ether derivatives. Using a relevant *in vitro* cellular model for blood-brain barrier integrity, we demonstrated that the compounds have a significant impact on the oxidative stress-resistance of the BBB. At low doses, compound **8** increased t-BHP-induced cellular damage while at a higher concentration it acted as a protective agent. Our results raise a warning that semi-synthetic modifications of cytoprotective ecdysteroids may unexpectedly alter their bioactivity profile towards harmful effects on cerebrovascular endothelial cells, which may confer them a central nervous system toxicity. The significance of these findings concerning phytoecdysteroid consumption is yet unclear and requires further studies.

Supporting information

S1 File.
(PDF)

Author Contributions

Conceptualization: Attila Hunyadi.

Data curation: Ana Raquel Santa-Maria, Judit P. Vigh, Fruzsina R. Walter, Gábor Tóth.

Funding acquisition: Fruzsina R. Walter, Mária A. Deli, Attila Hunyadi.

Investigation: Máté Vágvölgyi, Dávid Laczkó, Ana Raquel Santa-Maria, Judit P. Vigh, Fruzsina R. Walter, Róbert Berkecz, Gábor Tóth.

Resources: Mária A. Deli, Gábor Tóth, Attila Hunyadi.

Supervision: Mária A. Deli, Attila Hunyadi.

Writing – original draft: Máté Vágvölgyi, Dávid Laczkó, Gábor Tóth, Attila Hunyadi.

Writing – review & editing: Ana Raquel Santa-Maria, Fruzsina R. Walter, Mária A. Deli, Gábor Tóth, Attila Hunyadi.

References

1. Hu J, Luo CX, Chu WH, Shan YA, Qian Z-M, Zhu G, et al. 20-Hydroxyecdysone Protects against Oxidative Stress-Induced Neuronal Injury by Scavenging Free Radicals and Modulating NF-κB and JNK Pathways. PLOS ONE. 2012; 7(12):e50764. https://doi.org/10.1371/journal.pone.0050764 PMID: 23239983
2. Wang W, Wang T, Feng WY, Wang ZY, Cheng MS, Wang YJ. Ecdysterone protects gerbil brain from temporal global cerebral ischemia/reperfusion injury via preventing neuron apoptosis and deactivating astrocytes and microglia cells. Neurosci Res. 2014;81–82:21–9. Epub 20140127. https://doi.org/10.1016/j.neures.2014.01.005 PMID: 24480536
3. Tóth G, Santa-Maria AR, Herke I, Gáti T, Galvis-Montes D, Walter FR, et al. Highly Oxidized Ecdysteroids from a Commercial Cyanotis arachnoidea Root Extract as Potent Blood–Brain Barrier Protective

Agents. Journal of Natural Products. 2023; 86(4):1074–80. https://doi.org/10.1021/acs.jnatprod.2c00948 PMID: 36825873

4. Chung TD, Linville RM, Guo Z, Ye R, Jha R, Grifno GN, et al. Effects of acute and chronic oxidative stress on the blood-brain barrier in 2D and 3D in vitro models. Fluids Barriers CNS. 2022; 19(1):33. Epub 20220512. https://doi.org/10.1186/s12987-022-00327-x PMID: 35551622
5. Luceri C, Bigagli E, Femia AP, Caderni G, Giovannelli L, Lodovici M. Aging related changes in circulating reactive oxygen species (ROS) and protein carbonyls are indicative of liver oxidative injury. Toxicol Rep. 2018; 5:141–5. Epub 20171221. https://doi.org/10.1016/j.toxrep.2017.12.017 PMID: 29854585
6. Liguori I, Russo G, Curcio F, Bulli G, Aran L, Della-Morte D, et al. Oxidative stress, aging, and diseases. Clin Interv Aging. 2018; 13:757–72. Epub 20180426. https://doi.org/10.2147/CIA.S158513 PMID: 29731617
7. Song K, Li Y, Zhang H, An N, Wei Y, Wang L, et al. Oxidative Stress-Mediated Blood-Brain Barrier (BBB) Disruption in Neurological Diseases. Oxidative Medicine and Cellular Longevity. 2020; 2020:4356386. https://doi.org/10.1155/2020/4356386
8. Gorelick-Feldman J, Cohick W, Raskin I. Ecdysteroids elicit a rapid Ca^{2+} flux leading to Akt activation and increased protein synthesis in skeletal muscle cells. Steroids. 2010; 75(10):632–7. Epub 20100402. https://doi.org/10.1016/j.steroids.2010.03.008 PMID: 20363237
9. Csábi J, Hsieh TJ, Hasanpour F, Martins A, Kele Z, Gáti T, et al. Oxidized Metabolites of 20-Hydroxyecdysone and Their Activity on Skeletal Muscle Cells: Preparation of a Pair of Desmotropes with Opposite Bioactivities. J Nat Prod. 2015; 78(10):2339–45. Epub 20151014. https://doi.org/10.1021/acs.jnatprod.5b00249 PMID: 26465254
10. Issaadi HM, Csábi J, Hsieh TJ, Gáti T, Tóth G, Hunyadi A. Side-chain cleaved phytoecdysteroid metabolites as activators of protein kinase B. Bioorg Chem. 2019; 82:405–13. Epub 20181031. https://doi.org/10.1016/j.bioorg.2018.10.049 PMID: 30428419
11. Bogdán D, Haessner R, Vágvölgyi M, Passarella D, Hunyadi A, Gáti T, et al. Stereochemistry and complete ^{1}H and ^{13}C NMR signal assignment of C-20-oxime derivatives of posterone 2,3-acetonide in solution state. Magnetic Resonance in Chemistry. 2018; 56(9):859–66. https://doi.org/10.1002/mrc.4750 PMID: 29775488
12. Vágvölgyi M, Martins A, Kulmány A, Zupkó I, Gáti T, Simon A, et al. Nitrogen-containing ecdysteroid derivatives vs. multi-drug resistance in cancer: Preparation and antitumor activity of oximes, oxime ethers and a lactam. Eur J Med Chem. 2018; 144:730–9. Epub 2018/01/02. https://doi.org/10.1016/j.ejmech.2017.12.032 PMID: 29291440
13. Duddeck H, Dietrich W, Tóth G. Structure Elucidation by Modern NMR. Springer-Steinkopff: Darmstadt, 1998.
14. Pretsch E, Tóth G, Munk EM, Badertscher M. Computer-Aided Structure Elucidation. Wiley-VCH: Weinheim; 2002.
15. Weksler B, Romero IA, Couraud PO. The hCMEC/D3 cell line as a model of the human blood brain barrier. Fluids Barriers CNS. 2013; 10(1):16. Epub 20130326. https://doi.org/10.1186/2045-8118-10-16 PMID: 23531482
16. Weksler BB, Subileau EA, Perriere N, Charneau P, Holloway K, Leveque M, et al. Blood-brain barrier-specific properties of a human adult brain endothelial cell line. FASEB J. 2005; 19(13):1872–4. Epub 20050901. https://doi.org/10.1096/fj.04-3458fje PMID: 16141364
17. Veszelka S, Tóth A, Walter FR, Tóth AE, Gróf I, Mészáros M, et al. Comparison of a Rat Primary Cell-Based Blood-Brain Barrier Model With Epithelial and Brain Endothelial Cell Lines: Gene Expression and Drug Transport. Front Mol Neurosci. 2018; 11:166. Epub 20180522. https://doi.org/10.3389/fnmol.2018.00166 PMID: 29872378
18. Obermeier B, Daneman R, Ransohoff RM. Development, maintenance and disruption of the blood-brain barrier. Nat Med. 2013; 19(12):1584–96. Epub 20131205. https://doi.org/10.1038/nm.3407 PMID: 24309662
19. Kucera O, Endlicher R, Rousar T, Lotkova H, Garnol T, Drahota Z, et al. The effect of tert-butyl hydroperoxide-induced oxidative stress on lean and steatotic rat hepatocytes in vitro. Oxid Med Cell Longev. 2014; 2014:752506. Epub 20140331. https://doi.org/10.1155/2014/752506 PMID: 24847414
20. Harazin A, Bocsik A, Barna L, Kincses A, Váradi J, Fenyvesi F, et al. Protection of cultured brain endothelial cells from cytokine-induced damage by alpha-melanocyte stimulating hormone. PeerJ. 2018; 6:e4774. Epub 20180515. https://doi.org/10.7717/peerj.4774 PMID: 29780671
21. Santa-Maria AR, Walter FR, Valkai S, Bras AR, Mészáros M, Kincses A, et al. Lidocaine turns the surface charge of biological membranes more positive and changes the permeability of blood-brain barrier culture models. Biochim Biophys Acta Biomembr. 2019; 1861(9):1579–91. Epub 20190710. https://doi.org/10.1016/j.bbamem.2019.07.008 PMID: 31301276

22. Hunyadi A, Herke I, Lengyel K, Báthori M, Kele Z, Simon A, et al. Ecdysteroid-containing food supplements from Cyanotis arachnoidea on the European market: evidence for spinach product counterfeiting. Sci Rep. 2016; 6:37322. Epub 2016/12/09. https://doi.org/10.1038/srep37322 PMID: 27929032

23. Issaadi HM, Tsai Y-C, Chang F-R, Hunyadi A. Centrifugal partition chromatography in the isolation of minor ecdysteroids from Cyanotis arachnoidea. Journal of Chromatography B. 2017; 1054:44–9. https://doi.org/10.1016/j.jchromb.2017.03.043 PMID: 28419924

24. Kalari KR, Thompson KJ, Nair AA, Tang X, Bockol MA, Jhawar N, et al. BBBomics-Human Blood Brain Barrier Transcriptomics Hub. Front Neurosci. 2016; 10:71. Epub 20160301. https://doi.org/10.3389/fnins.2016.00071 PMID: 26973449

25. Walter FR, Veszelka S, Pásztói M, Péterfi ZA, Tóth A, Rákhely G, et al. Tesmilifene modifies brain endothelial functions and opens the blood-brain/blood-glioma barrier. J Neurochem. 2015; 134 (6):1040–54. Epub 20150723. https://doi.org/10.1111/jnc.13207 PMID: 26112237

26. Vigh JP, Kincses A, Ozgur B, Walter FR, Santa-Maria AR, Valkai S, et al. Transendothelial Electrical Resistance Measurement across the Blood-Brain Barrier: A Critical Review of Methods. Micromachines (Basel). 2021; 12(6). Epub 20210611. https://doi.org/10.3390/mi12060685 PMID: 34208338

27. Martin C, Martinez R, Navarro R, Ruiz-Sanz JI, Lacort M, Ruiz-Larrea MB. tert-Butyl hydroperoxide-induced lipid signaling in hepatocytes: involvement of glutathione and free radicals. Biochem Pharmacol. 2001; 62(6):705–12. https://doi.org/10.1016/s0006-2952(01)00704-3 PMID: 11551515

28. Zhao W, Feng H, Sun W, Liu K, Lu JJ, Chen X. Tert-butyl hydroperoxide (t-BHP) induced apoptosis and necroptosis in endothelial cells: Roles of NOX4 and mitochondrion. Redox Biol. 2017; 11:524–34. Epub 20170105. https://doi.org/10.1016/j.redox.2016.12.036 PMID: 28088644

29. Tóth AE, Walter FR, Bocsik A, Sántha P, Veszelka S, Nagy L, et al. Edaravone protects against methylglyoxal-induced barrier damage in human brain endothelial cells. PLoS One. 2014; 9(7):e100152. Epub 20140717. https://doi.org/10.1371/journal.pone.0100152 PMID: 25033388

30. Santa-Maria AR, Heymans M, Walter FR, Culot M, Gosselet F, Deli MA, et al. Transport Studies Using Blood-Brain Barrier In Vitro Models: A Critical Review and Guidelines. Handb Exp Pharmacol. 2022; 273:187–204. https://doi.org/10.1007/164_2020_394 PMID: 33037909